

*Supplementary information for*

# **Photocatalytic degradation of naproxen by H<sub>2</sub>O<sub>2</sub>-modified titanate nanomaterial under visible light irradiation**

Gongduan Fan<sup>a, b, \*</sup>, Jiajun Zhan<sup>a</sup>, Jing Luo<sup>a</sup>, Jin Zhang<sup>c</sup>, Zhong  
Chen<sup>a</sup>, Yifan You<sup>a</sup>

<sup>a</sup> *College of Civil Engineering, Fuzhou University, 350116 Fujian, China*

<sup>b</sup> *State Key Laboratory of Photocatalysis on Energy and Environment,  
Fuzhou University, 350002 Fujian, China*

<sup>c</sup> *Institute of Groundwater and Earth Sciences, Jinan University, 510632  
Guangzhou, China*

*\*Corresponding authors:*

Gongduan Fan, *E-mail: [fgdfz@fzu.edu.cn](mailto:fgdfz@fzu.edu.cn)*

## **1. The synthesis of TNM**

In a typical synthesis, 2 g of P25 powder was mixed with 12 mL of Milli-Q water (MQ) and 4 g of NaOH (final pH 13). Later on, the mixture was homogenized for 5 min under magnetic stirring and placed in a Teflon cell at 80°C for 24 h. After hydrothermal treatment, ion exchange ( $\text{Na}^+$  and  $\text{H}^+$ ) was conducted for 60 min by using 1 N HCl at the pH of 2 under magnetic stirring. Then the material was washed by Milli-Q water until pH 7. After that, the as-prepared samples were dried in oven at 100°C for 12 h and annealed at 550°C for 6 h to obtain the original titanate nanomaterial (TNM).

## **2. Photoreactor**

The photocatalytic degradation experiments were performed in a photochemical reactor as was shown in Fig. S1. It was equipped with a magnetic stirrer at a speed of 300 rad/min to ensure adequate reaction. A 500 W metal halogen lamp was used as the light source which combined with a UV cut-off filter and an infrared ray (IR) cut-off filter to remove wavelengths less than 400 nm and larger than 800 nm, respectively. A 250 mL sandwich beaker was used as the reactor, and the system was cooled by a circulating water bath to prevent the evaporation of water and maintained at room temperature. The distance between the lamp and the surface of solution was 15 cm. The intensity of light was 162 klux measured by a digital luxmeter (Jiading, JD-3, China).

## **3. Cycling experiments**

For the first cycle, 100 mL of 0.5 mg/L NPX solution was photocatalytic removed by 1.5 g/L of H<sub>2</sub>O<sub>2</sub>-modified titanate nanomaterials (HTNM) for 3 h under visible light irradiation. Later, after each cycle of the photocatalytic reaction, HTNM were separated and recycled from the solution by centrifugal collection, then washed thoroughly with deionized water to remove residual pollutants and dried in an oven at a temperature of 60°C, and the resulting nanocomposites were used in the succeeding.

#### **4. The analysis of PL spectra of HTNM photocatalyst**

In order to explore the defects exist in the HTNM photocatalyst and investigate the stability of HTNM from another side, PL spectra of the HTNM with/without usage excited by light with a wavelength of 362 nm were shown in Fig. S4. As shown in Fig. S4, a strong broad peak at 400–550 nm was observed for both HTNM samples, and multiple PL signals could be found in the visible region, which was mainly due to the excitonic emissions peaks of band edge free excitons and related to the traps on surface oxygen defects<sup>1, 2</sup>.

The emission peak at 412 nm could be attributed to the near band edge (NBE) transition<sup>3, 4</sup>. The occurrence of another defect related emission peak at 460 nm in case of HTNM was also reported by Jiang et al.<sup>1</sup>, and according to the previous studies, this emission (460 nm) was mainly attributed to excitonic PL emission which was due to surface states and defects<sup>5</sup>. In addition, the emission peak at 492 nm was also corresponding to intrinsic defects resulting from oxygen vacancies<sup>6</sup>. Furthermore, the emission peak observed around 514 nm could be assigned to vacancy-type defects such as oxygen vacancy and vacancy-combination defects<sup>1, 5</sup>, which could be easily

annealed out with relatively high temperatures. This PL result further supported the XPS results analyzed in section 3.1.5, that is, the existence of oxygen defects in HTNM played an important role in the process of photocatalytic degradation.

Moreover, according to previous studies, oxygen vacancies could easily bind photo-induced electrons to form excitons so that PL signal could easily occur, and the content of oxygen vacancy defects were corresponding to the PL signals<sup>1, 7, 8</sup>. Therefore, as can be seen from Fig. S4, compared with the initial HTNM, the PL signals of the HTNM had not changed much after photocatalytic degradation process, demonstrating that after photocatalytic degradation process, most of oxygen vacancies still existed in the HTNM, and made HTNM exhibit the excellent photocatalytic activity.

## **SUPPORTING FIGURE CAPTIONS**

**Fig. S1.** The schematic diagram of the experimental setup.

**Fig. S2.** (a) The XPS survey scans of HTNM photocatalyst; (b) and (c) The XPS patterns for the Ti 2p and O 1s core levels of HTNM photocatalyst before and after usage.

**Fig. S3.** The room-temperature photoluminescence spectra of HTNM photocatalyst before and after usage.

**Fig. S4.** HPLC mass spectrogram of NPX transformation samples.

**Fig. S5.** The mineralization of NPX during HTNM photocatalytic degradation process.

**Figure S1**

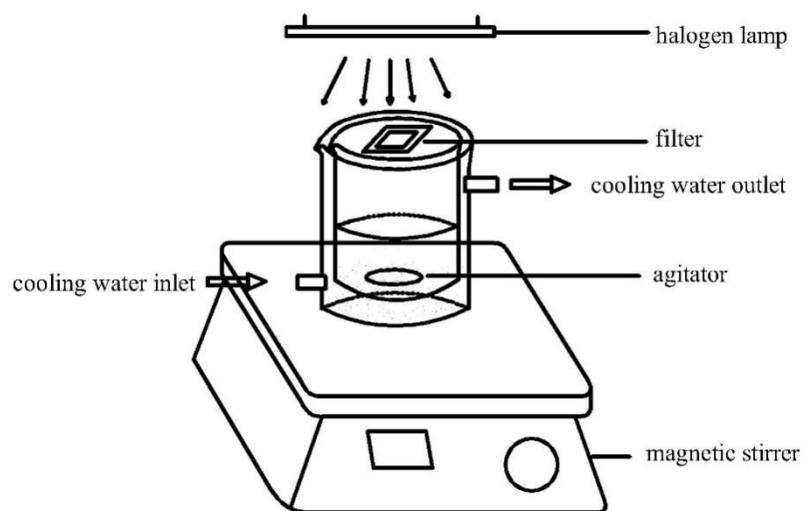


**Fig. S1.** The schematic diagram of the experimental setup.

Figure S2

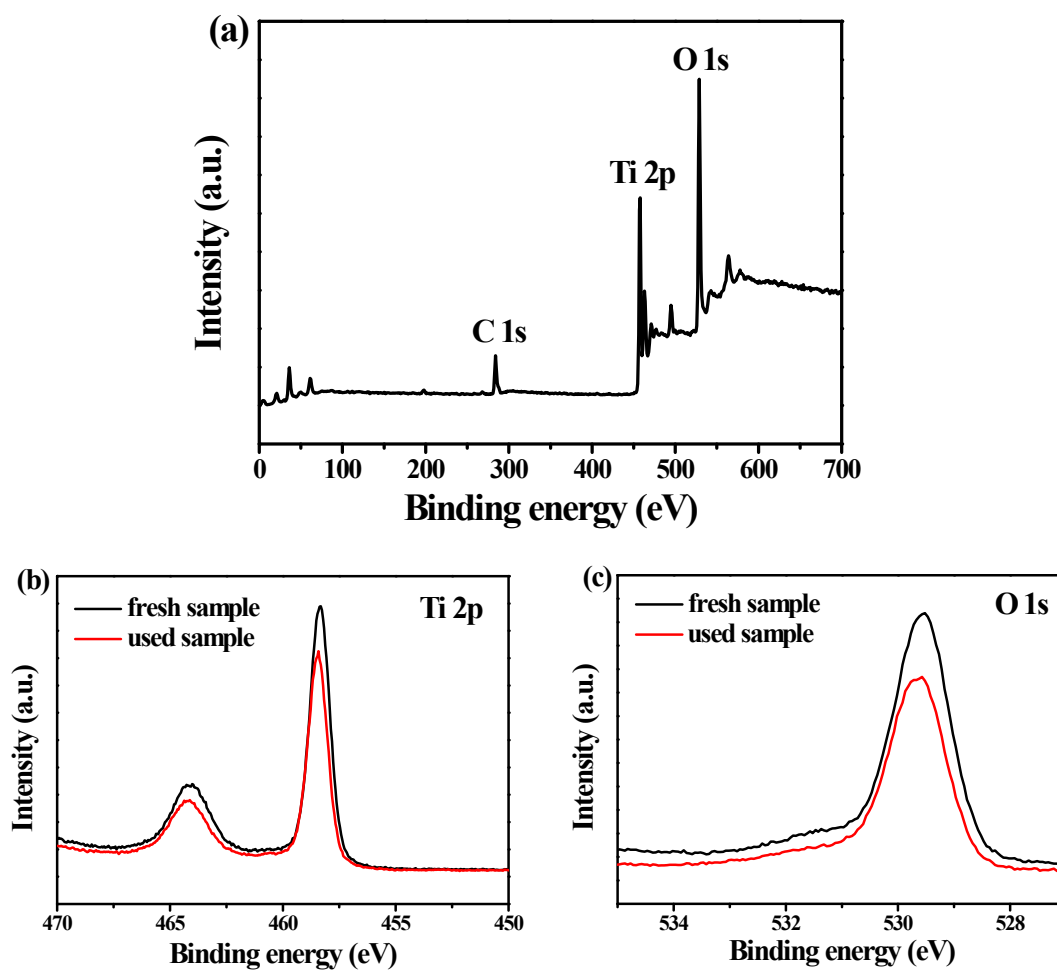


Fig. S2. (a) The XPS survey scans of HTNM photocatalyst; (b) and (c) The XPS patterns for the Ti 2p and O 1s core levels of HTNM photocatalyst before and after usage.

Figure S3

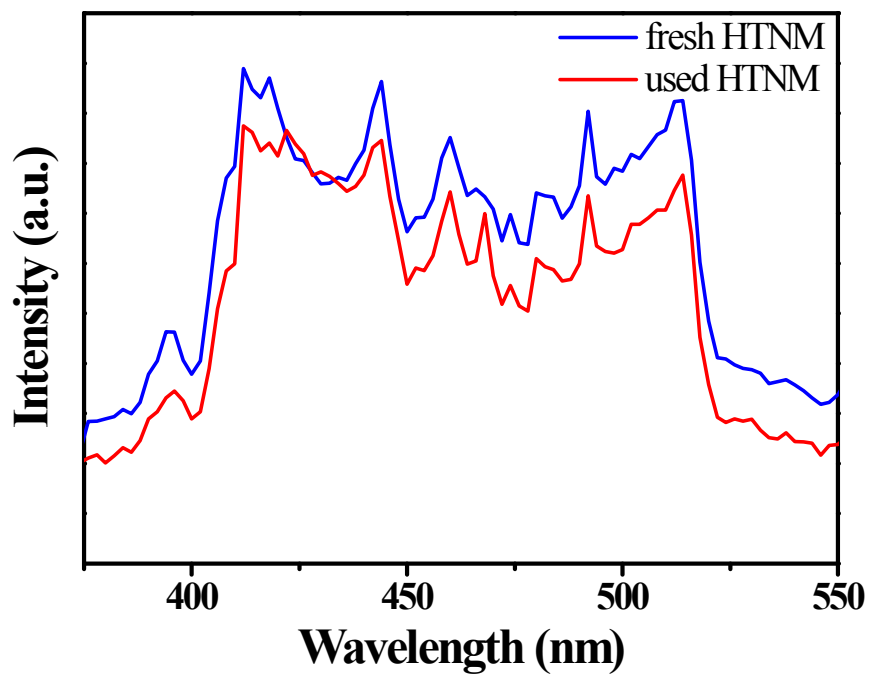
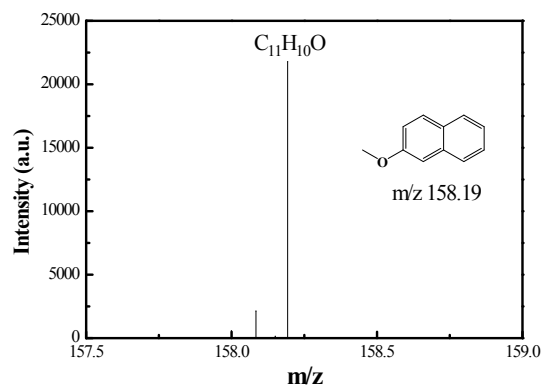


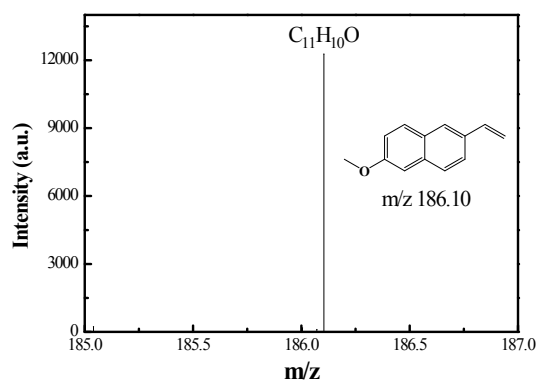
Fig. S3. The room-temperature photoluminescence spectra of HTNM photocatalyst before and after usage.



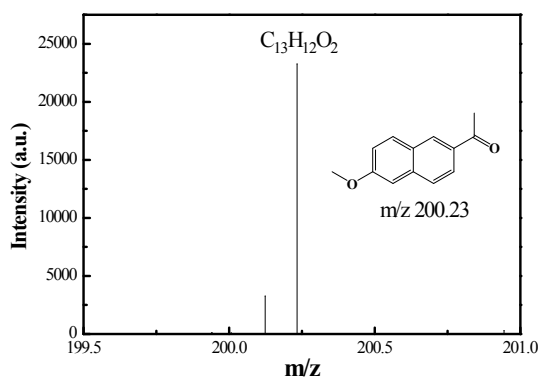
Figure S4



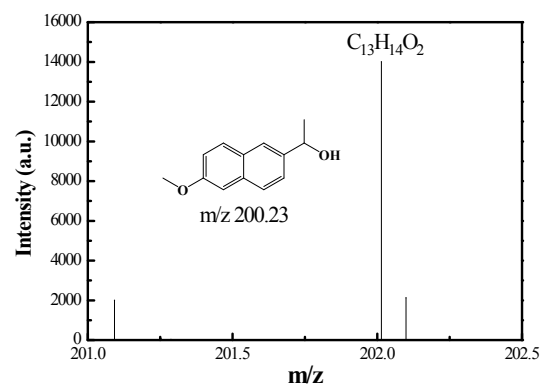
2-naphthyl methyl ether



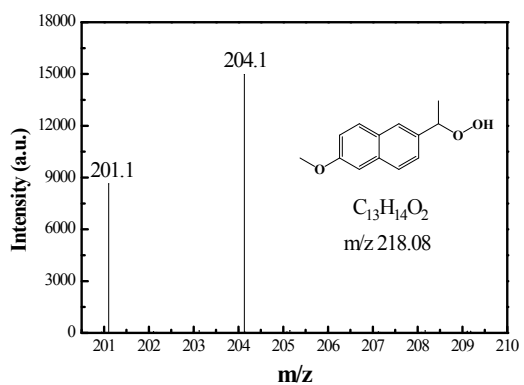
2-ethyl-6-methoxynaphthalene



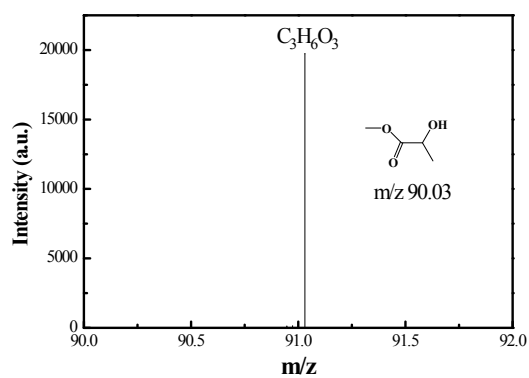
6-methoxy-2-acetylnaphthalene



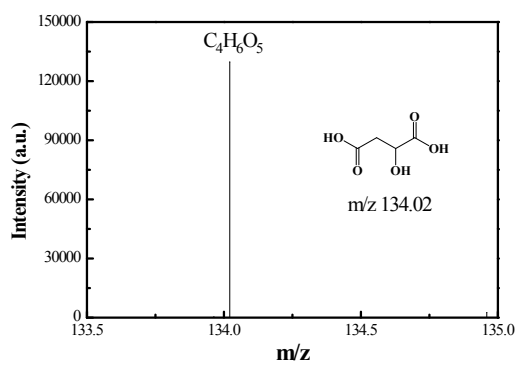
1-(6-methoxy-2-naphthyl methyl) ethanol



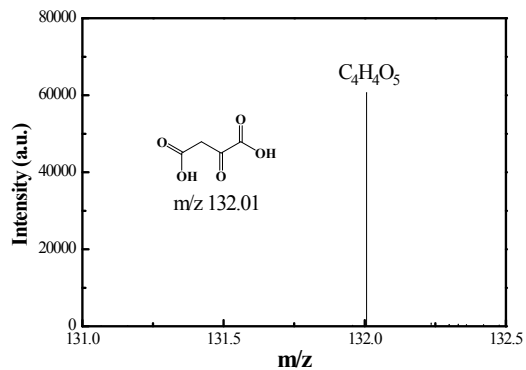
1-(6-methoxynaphthalene-2-yl)  
ethyl hydrogen peroxide



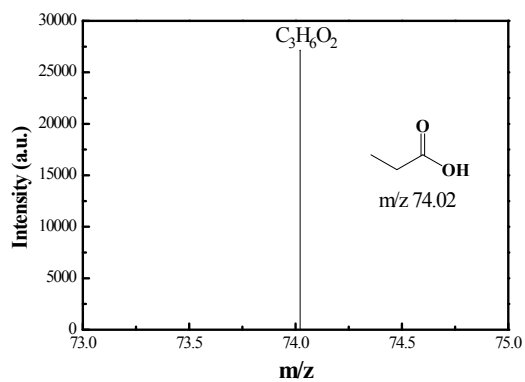
lactic acid



malic acid



acetoacetic acid



propionic acid

**Fig. S4.** HPLC mass spectrogram of NPX transformation samples.

Figure S5

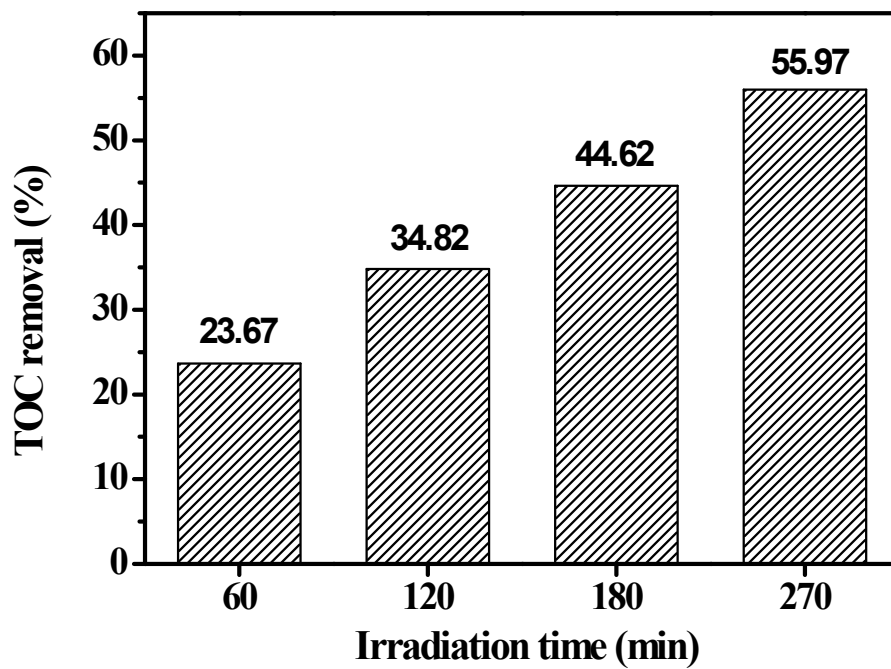


Fig. S5. The mineralization of NPX during HTNM photocatalytic degradation process.

## TABLES

**Table S1** Lattice parameters of TNM and HTNM photocatalysts

Photocatalyst	Peak position (2 $\theta$ )	FWHM	Crystal size (nm)	a (Å)	c (Å)
TNM	25.308	0.3683	20.79	3.784	9.515
HTNM	25.334	0.3732	20.51	3.780	9.510

**Table S2** Degradation kinetics of NPX under different conditions

Factors	Conditions	$R^2$	$k_{app}$ ( $\times 10^{-3} \text{ min}^{-1}$ )
NPX initial concentration ( $\text{mg L}^{-1}$ )	0.1	0.99024	$34.8 \pm 0.2474$
	0.5	0.98032	$43.9 \pm 0.4363$
	1.2	0.99471	$17.4 \pm 0.0855$
HTNM ( $\text{g L}^{-1}$ )	2	0.99132	$8.2 \pm 0.0536$
	0.5	0.98325	$33.9 \pm 0.4368$
	1.5	0.98028	$43.9 \pm 0.3484$
	2.5	0.97901	$13.6 \pm 0.1846$

## Reference

1. L. Jing, Q. Yichun, W. Baiqi, L. Shudan, J. Baojiang, Y. Libin, F. Wei, F. Honggang and S. Jiazhong, *Solar Energy Materials Solar Cells*, 2006, **90**, 1773-1787.
2. L. Kernazhitsky, V. Shymanovska, T. Gavrillo, V. Naumov, L. Fedorenko, V. Kshnyakin and J. Baran, *Journal of Luminescence*, 2014, **146**, 199-204.
3. Y. Liu and R. O. Claus, *Journal of the American Chemical Society*, 1997, **119**, 5273-5274.
4. A. H. Yuwono, Y. Zhang, J. Wang, X. H. Zhang, H. Fan and W. Ji, *Chemistry of Materials*, 2016, **18**, 5876-5889.
5. B. Liu, L. Wen and X. Zhao, *Materials Chemistry Physics*, 2007, **106**, 350-353.
6. J. Dhanalakshmi, S. Iyyapushpam, S. T. Nishanthi, M. Malligavathy and D. Pathinettam Padiyan, *Advances in Natural Sciences Nanoscience Nanotechnology*, 2017, **8**, 15-15.
7. L. Jing, S. Xiaojun, X. Baifu, W. Baiqi, C. Weimin and F. Honggang, *Journal of Solid State Chemistry*, 2004, **177**, 3375-3382.
8. D. K. Pallotti, L. Passoni, P. Maddalena, F. D. Fonzo and S. Lettieri, *Journal of Physical Chemistry C*, 2017, **121**, 9011-9021.